Journal of Power Sources 227 (2013) 48–52

Contents lists available at SciVerse ScienceDirect

Journal of Power Sources

journal homepage: www.elsevier.com/locate/jpowsour

Short communication

$Sm_{0.5}Sr_{0.5}CoO_{3-\delta}$ – A new bi-functional catalyst for rechargeable metal-air battery applications

S. Velraj, J.H. Zhu*

Department of Mechanical Engineering, Tennessee Technological University, TN – 38501, United States

HIGHLIGHTS

- $Sm_{0.5}Sr_{0.5}CoO_{3-\delta}$ (SSC) was proposed and evaluated as a new bifunctional catalyst.
- SSC and $La_{0.6}Ca_{0.4}CoO_3$ (LCC) catalysts had similar electrochemical performance.
- The SSC electrodes had a longer lifetime over the LCC electrodes.
- The degradation mechanisms were different for these two electrodes.

ARTICLE INFO

Article history:
Received 24 July 2012
Received in revised form
24 October 2012
Accepted 13 November 2012
Available online 20 November 2012

Keywords:
Perovskite
Bi-functional electrode
Metal-air battery
Oxygen reduction
Oxygen evolution
Cyclic life

ABSTRACT

$Sm_{0.5}Sr_{0.5}CoO_{3-\delta}$ (SSC) was evaluated as a bi-functional catalyst for rechargeable metal-air battery cathodes. The catalyst was homogenously dispersed on corrosion-resistant graphitized Vulcan XC-72R carbon powder for the cathode fabrication. For comparison, the air cathode catalyzed with the widely studied perovskite $La_{0.6}Ca_{0.4}CoO_3$ (LCC) was included in the evaluation. Based on the polarization curves, SSC exhibited similar catalytic activities as LCC for both oxygen evolution reaction and oxygen reduction reaction. Furthermore, the air cathode prepared with SSC exhibited an improved cyclic life. These results suggest that SSC is a promising alternative to LCC as a bi-functional catalyst for metal-air battery cathode applications.

1. Introduction

A renewed interest in clean and renewable intermittent power sources like wind, solar and tide has sparked a need for better energy storage devices. In theory, rechargeable metal-air battery with its high energy storage capacity and environment-friendly materials provides one of the most promising solutions [1]. However, the air cathodes of rechargeable metal-air batteries have the issue of irreversibility of the oxygen evolution and reduction reactions [2]. Noble metal/noble metal alloys have shown good bi-functional capabilities but have been unfavorable mainly for economical reasons [3–5]. The non-noble alternatives are perovskites, spinels and pyrochlores [6–9]. Among them, perovskites with the chemical formula of ABO_3 have been studied extensively and have recently received increasing attention, due to their higher electrochemical performance and lifetime in the alkaline electrolyte [2,10,11]. Ca-doped $LaCoO_3$, especially $La_{0.6}Ca_{0.4}CoO_3$ (LCC), has so far been the most promising bi-functional catalyst and has been widely used in demonstration cells [12–14].

Sr-doped Sm cobaltite – $Sm_{0.5}Sr_{0.5}CoO_{3-\delta}$ (SSC), which has been used as an oxygen reduction catalyst for solid oxide fuel cell (SOFC) cathode [15–17], might also possess bi-functional catalytic activities desirable for metal-air battery cathode application. In this work, we attempt to assess the prospective of SSC as a bi-functional catalyst in the air cathode by investigating the electrochemical performance in terms of oxygen reduction reaction (ORR), oxygen evolution reaction (OER), as well as cyclic life. Since the carbon support used for catalyst dispersion has a huge impact on the overall activity and stability of the electrode [18], SSC was dispersed on the corrosion-resistant graphitized Vulcan XC-72R for cathode fabrication. Air cathodes were also fabricated with LCC as catalyst to benchmark the performance of the new SSC catalyst. Furthermore,

* Corresponding author. Tel.: +1 931 372 3186; fax: +1 931 372 6340.
E-mail address: jzhu@tntech.edu (J.H. Zhu).

0378-7753/$ – see front matter © 2012 Elsevier B.V. All rights reserved.
http://dx.doi.org/10.1016/j.jpowsour.2012.11.031

a control cathode using only the graphitized Vulcan XC-72R with no SSC or LCC added in the active layer was prepared and included in the evaluation to obtain the baseline performance of the carbon support.

2. Experimental

2.1. Catalyst and carbon support

The SSC nano-powder (from Sigma–Aldrich) was used as-received. LCC was synthesized by the glycine nitrate process (GNP). In this process, aqueous solutions of $La(NO_3)_3$, $Ca(NO_3)_2$, and $Co(NO_3)_2$ (from Alfa Aesar) were prepared separately and mixed to form a solution with the addition of a desired amount of glycine as fuel. The solution was heated at 350 °C, subsequently evaporating the water until it formed a gel that auto-ignited to form ash. The collected ash was ground and then calcined at 650 °C for 2 h in a stagnant air furnace to form the LCC powder. The phase structure and particle size of both the SSC and LCC powders were characterized by X-ray diffraction (XRD) and scanning electron microscopy (SEM).

The carbon support used in this study was a treated Vulcan XC-72R carbon powder. After graphitizing the as-received Vulcan XC-72R at 2700 °C to improve its corrosion resistance, the powder was heat treated at 600 °C in air to enable a weight loss of 10% via oxidation for increasing the activity for the ORR. It has been found that the graphitization of carbon powder enhanced its corrosion resistance [19].

2.2. Electrode preparation

The air cathode consisted of a gas diffusion layer, an Ni-mesh current collector and an active layer. The hydrophobic diffusion layer was prepared by ball milling a 30 wt% diluted polytetrafluoroethylene (PTFE) suspension with 70 wt% acetylene black to form a slurry which was then dried for 12 h at 80 °C. To prepare the semi-hydrophobic active layer loaded with the perovskite catalyst, 45 wt% carbon black powder and 35 wt% catalyst (SSC or LCC) were ultrasonically agitated in excess 2-propanol/H_2O (1:1) for 15 min followed by 25-min mechanical mixing. 20 wt% diluted PTFE suspension was then added into the mixture drop-by-drop while the mixture was being stirred. The agitation-mixing process was repeated once to uniformly disperse the three constituents. The slurry was filtered and dried for 12 h at 80 °C. For preparing the active layer used in the control cathode, no perovskite catalyst was added and the amount of the carbon black powder was increased to 80 wt%. Both the dried powders for the active and diffusion layers were kneaded with 2-propanol to form doughs which were rolled in several steps to thin sheets of 0.25 and 0.4 mm, respectively. The Ni 200-mesh current collector was placed between the active and gas diffusion layers, and the assembly was pressed at 340 °C for 30 min under 40 kg cm^{-2} to form a bonded cathode.

2.3. Electrochemical testing

The prepared cathodes were tested in a three-electrode arrangement. All measurements were carried out at ambient temperature in air with 2.85-cm^2 air electrodes in an 8.5 M KOH electrolyte. A platinum mesh (2 cm^2) and an Hg/HgO electrode were used as counter and reference electrodes, respectively. The half cell was rested for 48 h to assure that the electrolyte had sufficient time to penetrate into the structure of the active layer. The polarization curves were then obtained at 0.5 mV s^{-1}. For cyclic life tests, one full cycle consisted of both processes (0.5 h of cathodic and 0.5 h of anodic operation). The anodic and cathodic current densities used during testing were +/− 53 mA cm^{-2}. After each half-cycle, a rest of 0.5 h occurred. Before and after cyclic life testing, the impedance spectra were measured potentiostatically when the current density had reached a steady state with a Gamry Reference 3000. The frequency range was from 100 kHz to 10 mHz, so that all faradic processes were included. None of the measurements were compensated for IR-drops.

3. Results and discussion

3.1. Characterization of SSC and LCC

The XRD patterns for the two perovskite catalysts are shown in Fig. 1. In Fig. 1a, the SSC powder exhibited strong peaks corresponding to a perovskite phase with additional second-phase peaks (identified as $SrCoO_{3-x}$ with a monoclinic structure, about 8 wt% in the powder), while the LCC powder was single-phase as indicated in Fig. 1b. It should be noted that it was very difficult to achieve a phase-pure SSC powder, as there was always some type of residual second phase co-existing with the SSC phase after calcination of the as-received SSC powder at different temperatures in air. It is also worth mentioning that the small quantity of the second phase $SrCoO_{3-x}$ did not affect the overall performance of the catalyst, as a cathode prepared using the SSC catalyst that contained a small amount of Co_3O_4 and was free of the $SrCoO_{3-x}$ phase had the same electrochemical properties and cyclic lifetime as the SSC cathode used in this study (not reported in the paper).

The SSC powder had a primary particle size of around 50 nm in diameter according to the manufacturer's specifications as well as the SEM image as shown in Fig. 2a and b. The LCC powder prepared by the GNP process also had a nanoporous structure as shown in Fig. 2c and d. The particle size of the LCC powder was calculated to be 23 nm, based on the XRD peak broadening analysis [20].

3.2. Electrochemical characterization

It has been found that the electrochemical performance and cycle lifetime of an air cathode depend on the surface area, crystallinity and wettability of the carbon support used [21]. A detailed study on carbon supports revealed that the as-received Vulcan and the treated one (i.e. graphitized and activated Vulcan with 10% weight loss) had a surface area of 250 and 100 $m^2\ g^{-1}$, respectively [18]. It was also shown that the untreated Vulcan had the highest

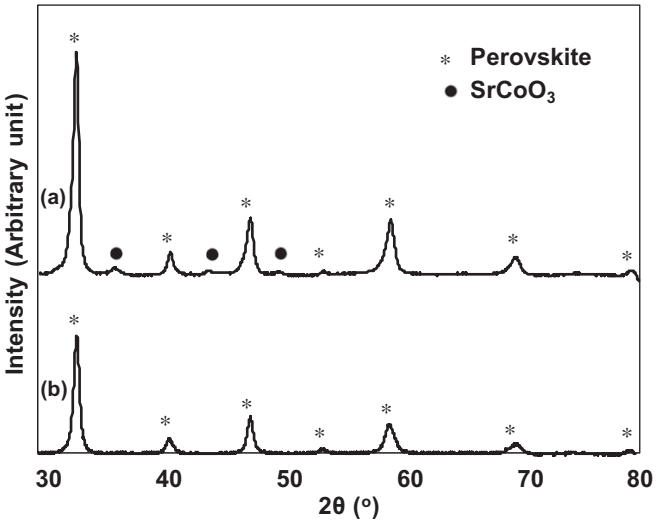

Fig. 1. XRD patterns of the two catalysts: (a) SSC and (b) LCC.

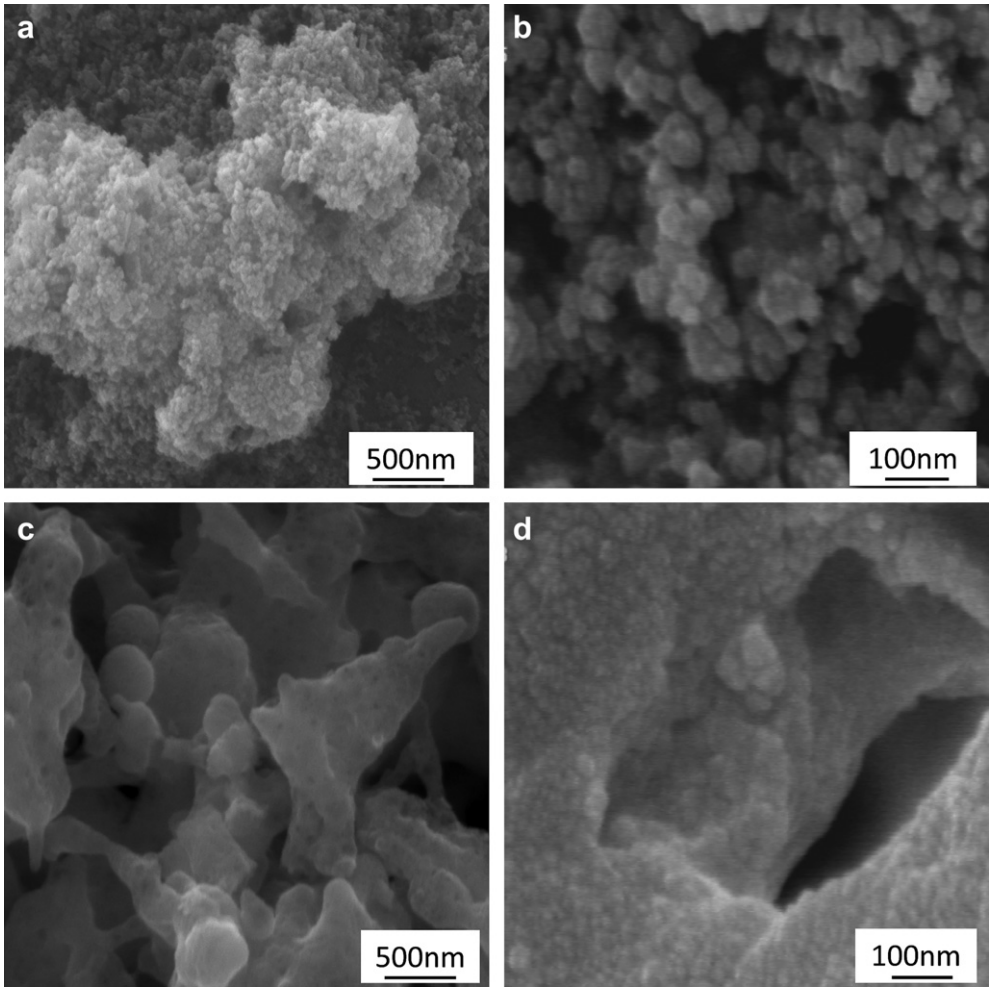

Fig. 2. SEM images of the catalyst powders at different magnifications: (a) and (b) SSC; (c) and (d) LCC.

oxygen reduction activity but the treated one had the longest lifetime. In this paper, the treated Vulcan was used as the catalyst support to maximize the cycle lifetime of the cathodes. Fig. 3 shows the cathodic polarization curves for the control, SSC and LCC cathodes. The cathodic polarization curves of the two catalysts were similar (e.g., 175 ± 10 mA cm^{-2} at 0.4 V), revealing the competitive catalytic activity for the ORR of SSC in comparison with LCC. Fig. 4 shows the anodic polarization curves for the three

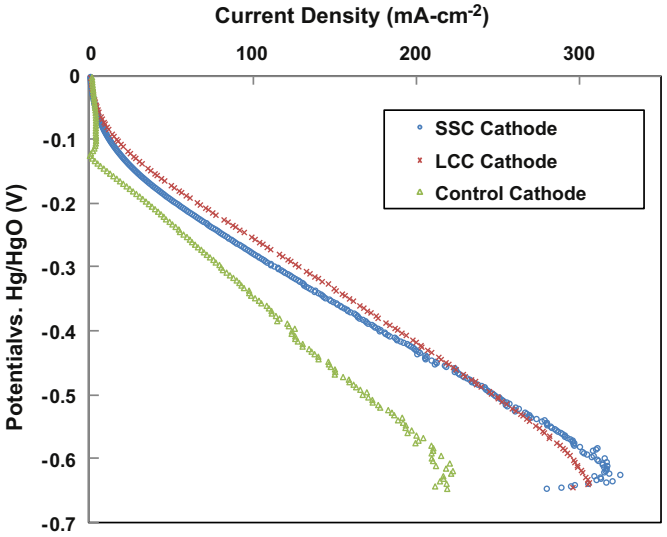

Fig. 3. Cathodic polarization curves of the electrodes prepared with the SSC and LCC catalysts as well as the control cathode.

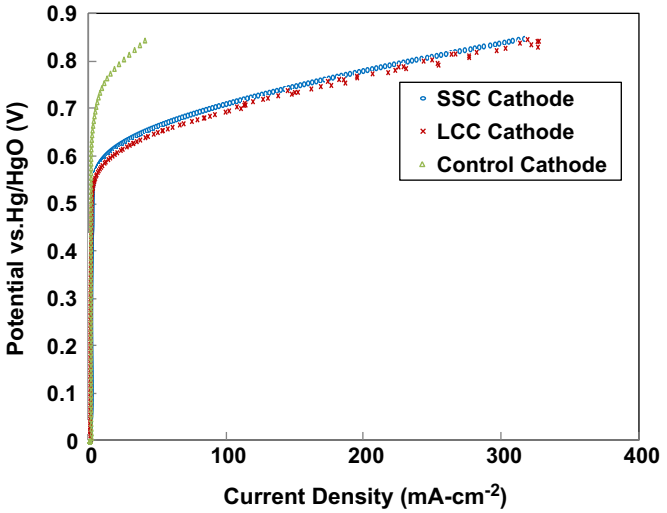

Fig. 4. Anodic polarization curves of the electrodes prepared with the SSC and LCC catalysts as well as the control cathode.

cathodes. Again, no significant difference in overpotential was observed for the OER taking place on the perovskite in the electrodes, irrespective of the catalyst used. It is evident from the polarization curves that the new catalyst SSC has impressive bi-functional capabilities, comparable to LCC. The cathodic and anodic polarization curves of the control cathode are also shown in Figs. 3 and 4. The control cathode had reasonable activity for the ORR due to oxygen reduction on carbon to form hydrogen peroxide [13]. However, as indicated in Fig. 4, the anodic polarization curve of the control cathode revealed no significant anodic activity over the measured potential range, as expected for the carbon support.

3.3. Cyclic life evaluation

To further evaluate the bi-functionality and stability of SSC in comparison with LCC, the air electrodes were subject to cycles of oxygen reduction and evolution under the current density of 53 mA cm^{-2}. Since the OER capability of the control cathode was very poor, a meaningful cyclic test was not feasible. According to Fig. 5, the cathode with the SSC catalyst exhibited a much longer lifetime (106 cycles at −0.3 V) than that with LCC (68 cycles at −0.3 V), implying the superior lifetime characteristics of the SSC catalyst. The SSC cathode had a relatively stable potential for both ORR and OER up to around 85 cycles, followed by an accelerated degradation period (Fig. 5). Since the diffusion layer side of the electrodes were exposed to ambient air, the degradation could be ascribed to the damage in the electrode due to carbon oxidation and subsequent carbonate formation during oxygen evolution reaction [22,23]. Also, cracks were evident in the active layer for the SSC cathode due to the damage (and also possibly pressure increase) during oxygen evolution and eventual mechanical degradation of the electrode [21]. The general trend of electrode failure is the final rapid degradation which starts with the OER and continues for the ORR. This trend is noted by the increase in OER overpotential followed by an increase in ORR overpotential as well as the presence of cracks in the active layer of the electrode.

For the LCC cathodes, the number of cycles for each period was drastically reduced along with the total lifetime. Interestingly, the final degradation of the LCC cathode was different from the SSC cathode without an increase in the OER voltage (Fig. 5) and also without visible cracks on the electrode even though the ORR potential increased drastically. Furthermore, some of the LCC particles were apparently detached from the electrode, as loose particles could be detected on the tested electrode as well as in the electrolyte solution. This failure mode could be due to the loss of ORR catalytic activity of the LCC catalyst and/or the detachment of LCC from the electrode, rather than the mechanical degradation as observed for the SSC cathode.

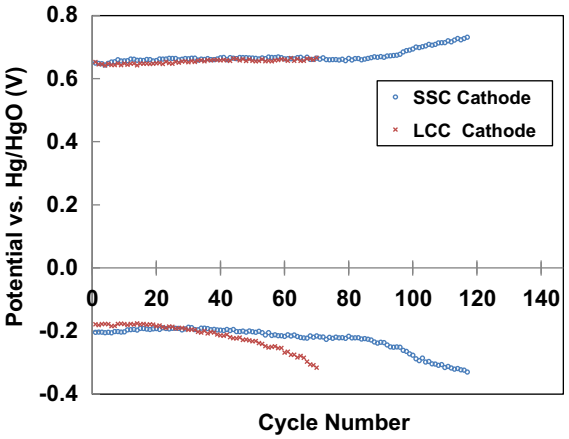

Fig. 5. Cycle life performance of the electrodes catalyzed with SSC and LCC with a current density of 53 mA cm^{-2}. One full cycle consisted of 0.5 h of cathodic and 0.5 h of anodic operation with a 0.5 h rest in between.

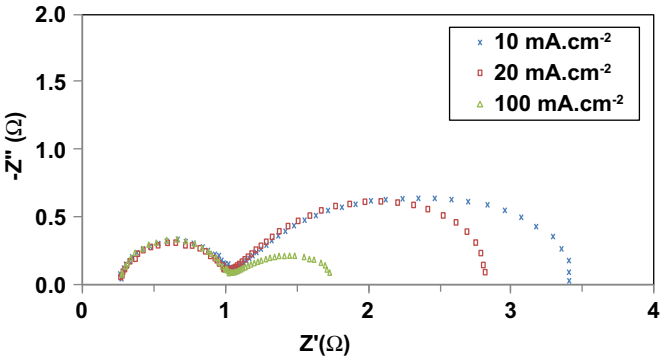

Fig. 6. Nyquist plot for the electrode with the SSC catalyst dispersed on the treated Vulcan after cyclic life test. The impedance spectra were measured at different cathodic current densities in ambient air with an 8.5 M KOH electrolyte.

AC impedance spectroscopy has been effectively used to investigate the kinetics, diffusion and adsorption features of air electrodes [24,25]. The impedance spectroscopic characteristics of the electrodes catalyzed by both the SSC and LCC catalysts were investigated at different cathodic current densities (10, 20 and 100 mA cm^{-2}), before and after the cyclic test. For all the tested cathodes, two distinctive semicircles existed in the frequency range from 100 kHz to 100 mHz. As an example, Fig. 6 shows the impedance spectra obtained for the SSC cathode after cycling at different cathodic current densities. Since the size of the high-frequency semicircle remained unchanged as the cathodic current density increased, this portion of the impedance was ascribed to distributed resistances inside the porous structure [23]. The size of the low-frequency semicircle, which was related to kinetic impedance of ORR, decreased with the increase in current density [23,26]. Nyquist plots of the electrode with the SSC catalyst before and after cycling at a cathodic current density of 10 mA cm^{-2} are shown in Fig. 7. The distributed resistances of the electrode increased from 0.15 to 1.0 Ω after cycling while the kinetic resistance increased only slightly from 2.25 to 2.3 Ω. This increase in distributed resistances of the electrode after cyclic testing might be due to the already mentioned damage and cracks in the active layer of the electrode. As shown in Fig. 8, for the electrode with the LCC catalyst, the distributed resistances of the electrode increased from

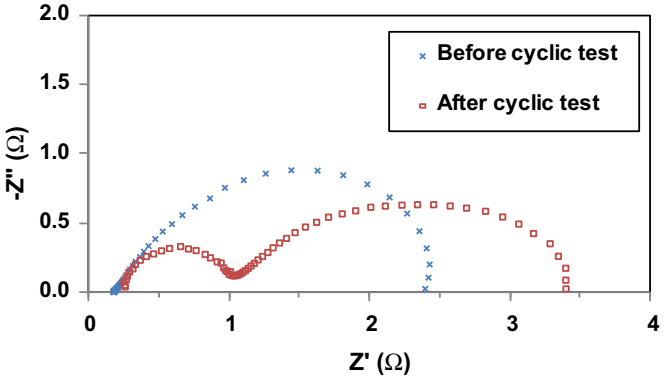

Fig. 7. Nyquist plot for the electrode with the SSC catalyst dispersed on the treated Vulcan before and after cyclic life test. The impedance spectra were measured at a cathodic current density of 10 mA cm^{-2} in ambient air with an 8.5 M KOH electrolyte.

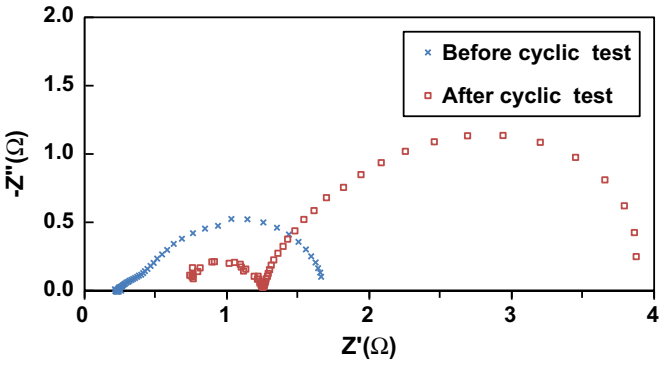

Fig. 8. Nyquist plot for the electrode with the LCC catalyst dispersed on the treated Vulcan before and after cyclic life test. The impedance spectra were measured at a cathodic current density of 10 mA cm^{-2} in ambient air with an 8.5 M KOH electrolyte.

0.35 to 0.55 Ω after cycling while the kinetic resistance increased from 1.30 to 2.6 Ω. There was also an increase in the electrolyte/contact resistance (i.e. the intersection of the spectrum with the *X*-axis on the high-frequency side) of about 0.5 Ω after cyclic test for the LCC electrode, while no such change was noticed for the SSC electrode (Fig. 7). Such simultaneous increase in the electrolyte/contact, distributed, and kinetic resistances may be related to the dissolution/detachment of the LCC catalyst into the electrolyte observed after cyclic testing for this electrode.

4. Conclusions

Air electrodes were prepared with both SSC and LCC as catalysts on the treated Vulcan XC-72R support. Based on the polarization curves, the SSC and LCC catalysts had similar electrochemical performance and catalytic activity for both ORR and OER. Results from cycle life tests indicated that the cycle lifetime of the SSC electrode was significantly longer than that of the LCC electrode and the failure modes of these two cathodes were significantly different. Overall, SSC has been shown to have high bi-functional catalytic activity that is stable and sustainable for potential application in metal-air batteries.

Acknowledgment

This research was supported by Tennessee Technological University (TTU) through a Faculty Research Grant. The authors also wish to thank the Center for Manufacturing Research, TTU, for providing additional research funding.

References

[1] M. Jacoby, Chem. Eng. News Arch. 88 (2010) 29–31.
[2] L. Jörissen, J. Power Sources 155 (2006) 23–32.
[3] Y.-C. Lu, Z. Xu, H.A. Gasteiger, S. Chen, K. Hamad-Schifferli, Y. Shao-Horn, J. Am. Chem. Soc. 132 (2010) 12170–12171.
[4] H.-K. Lee, J.-P. Shim, M.-J. Shim, S.-W. Kim, J.-S. Lee, Mater. Chem. Phys. 45 (1996) 238–242.
[5] B.C. Beard, J. Electrochem. Soc. 137 (1990) 3368–3374.
[6] G. Roberts, Rev. Process. Chem. Eng. 3 (2000) 151–174.
[7] J.O. Bockris, T. Otagawa, J. Electrochem. Soc. 131 (1984) 290–302.
[8] F. Švegl, B. Orel, I. Grabec-Švegl, V. Kaučič, Electrochim. Acta 45 (2000) 4359–4371.
[9] A.K. Shukla, A.M. Kannan, M.S. Hegde, J. Gopalakrishnan, J. Power Sources 35 (1991) 163–173.
[10] F. Bidault, D.J.L. Brett, P.H. Middleton, N.P. Brandon, J. Power Sources 187 (2009) 39–48.
[11] J. Suntivich, K.J. May, H.A. Gasteiger, J.B. Goodenough, Y. Shao-Horn, Science 334 (2011) 1383–1385.
[12] S. Müller, K. Striebel, O. Haas, Electrochim. Acta 39 (1994) 1661–1668.
[13] Y. Shimizu, K. Uemura, H. Matsuda, N. Miura, N. Yamazoe, J. Electrochem. Soc. 137 (1990) 3430–3433.
[14] S.-W. Eom, S.-Y. Ahn, I.-J. Kim, Y.-K. Sun, H.-S. Kim, J. Electroceram. 23 (2009) 382–386.
[15] S.W. Baek, J.H. Kim, J. Bae, Solid State Ionics 179 (2008) 1570–1574.
[16] H. Zhang, H. Liu, Y. Cong, W. Yang, J. Power Sources 185 (2008) 129–135.
[17] Z. Gao, X. Liu, B. Bergman, Z. Zhao, J. Power Sources 196 (2011) 9195–9203.
[18] S. Müller, F. Holzer, H. Arai, O. Haas, J. New Mater. Electrochem. Syst. (1999) 227–232.
[19] P.N. Ross, M. Sattler, J. Electrochem. Soc. 135 (1988) 1464–1470.
[20] C. Suryanarayana, M.G. Norton, X-ray Diffraction: A Practical Approach, Plenum Press, New York, 1998.
[21] H. Arai, S. Müller, O. Haas, J. Electrochem. Soc. 147 (2000) 3584–3591.
[22] M. Bursell, M. Pirjamali, Y. Kiros, Electrochim. Acta 47 (2002) 1651–1660.
[23] S. Zhuang, K. Huang, C. Huang, H. Huang, S. Liu, M. Fan, J. Power Sources 196 (2011) 4019–4025.
[24] F. Alcaide, E. Brillas, P.-L. Cabot, J. Electroanal. Chem. 547 (2003) 61–73.
[25] N. Wagner, K.A. Friedrich, Fuel Cells 9 (2009) 237–246.
[26] H. Huang, W. Zhang, M. Li, Y. Gan, J. Chen, Y. Kuang, J. Colloid Interface Sci. 284 (2005) 593–599.